Available online at www.sciencedirect.com
ScienceDirect
International Journal of Multiphase Flow 32 (2006) 1141–1159
International Journal of Multiphase Flow
www.elsevier.com/locate/ijmulflow

Periodic boiling in parallel micro-channels at low vapor quality

G. Hetsroni *, A. Mosyak, E. Pogrebnyak, Z. Segal

Department of Mechanical Engineering, Technion-Israel Institute of Technology, Haifa 32000, Israel

Received 15 November 2005; received in revised form 15 June 2006

Abstract

Based on experimental investigations the present study evaluates instability and heat transfer phenomenon under condition of periodic flow boiling of water and ethanol in parallel triangular micro-channels. Tests were performed in the range of hydraulic diameter 100–220 μm, mass flux 32–200 kg/m^2 s, heat flux 120–270 kW/m^2, vapor quality $x = 0.01$–0.08. The period between successive events depends on the boiling number and decreases with an increase in the boiling number. The initial film thickness decreases with increasing heat flux. When the liquid film reached the minimum initial film thickness CHF regime occurred. Temporal variations of pressure drop, fluid and heater temperatures were periodic. Oscillation frequency is the same for the pressure drop, for the fluid temperature at the outlet manifold, and for the mean and maximum heater temperature fluctuations. All these fluctuations are in phase. The CHF phenomenon is different from that observed in a single channel of conventional size. A key difference between micro-channel heat sink and single conventional channel is amplification of parallel-channel instability prior to CHF. The dimensionless experimental values of the heat transfer coefficient are presented as the Nusselt number dependence on the Eotvos number and the boiling number.

Keywords: Micro-channel; Boiling; Instability; Explosive regime; Heat transfer; Dryout

1. Introduction

Micro-channel heat sinks are devices that provide liquid or two-phase flow through parallel channels of diameter less than 1 mm. These systems are ideally suited for devices where high heat flux is dissipated from small surface area of high performance supercomputers, optical devices, electric vehicles and advanced military avionics. Phase-change processes, particularly flow boiling, are important in the micro-scale and significant work has been done in this area. The extend to which an incoming liquid will be vaporized is a design variable that depends upon the intended application. In micro-scale refrigeration systems, the change in vapor quality may be substantial, on the order of 0.8, for example. In electronic cooling applications, the equilibrium vapor quality may remain at zero or be very small to capture the high heat transfer coefficients of subcooled

* Corresponding author. Tel.: +972 48 292058; fax: +972 48 238101.
E-mail address: hetsroni@technix.technion.ac.il (G. Hetsroni).

0301-9322/$ - see front matter © 2006 Elsevier Ltd. All rights reserved.
doi:10.1016/j.ijmultiphaseflow.2006.06.005

flow boiling without the need to incorporate a condenser, (Bergles et al., 2003). The hydraulic diameter of micro-channels, d_h, is in the range 10–500 μm, the length, L, is in the range 10–15 mm. Assuming that the channels are cut from one side, a cover plate is provided on that side, whereas heat is usually applied to the opposite side, and inlet and outlet manifolds connect the micro-channel heat exchanger to the flow system. The pressure drop is kept at a reasonable level, so that the boiling in the micro-channels occurs at low Reynolds numbers. The modeling of flow boiling in micro-channels at low vapor quality and low Reynolds numbers has not received much attention in the literature.

Kandlikar (2004), Kandlikar and Balasubramanian (2004) presented the flow boiling correlations to transition, laminar and deep laminar flows in micro-channels. The flow boiling correlations for large diameter tubes developed by Kandlikar (1990) were modified for flow boiling in micro-channels. The correlations were extended to laminar flow in micro-channels at $Re < 100$ and compared to experimental data of Yen et al. (2003) for single tube of diameter 0.19 mm. Based on the data-set, it was concluded that boiling was more nucleate dominant for low Reynolds numbers ($Re < 100$) in micro-channels. The correlations proposed were verified for refrigerants as coolant in the range of Reynolds number $Re = 72$–1490. They were not verified for water flow. The liquid film formation was proposed as a key parameter that affects heat transfer coefficient in the models of saturated boiling in micro-channels.

Qu and Mudawar (2003a) presented and discussed experimental results, which provide physical insight into the unique nature of saturated flow boiling heat transfer in a water-cooled micro-channel heat sink. Contrary to macro-channel the heat transfer coefficient was shown to decrease with increasing thermodynamic equilibrium quality. This unique trend was attributed to appreciable droplet entrainment and onset of annular flow regime development. Such a trend of heat transfer coefficient at low vapor quality was also reported by Hetsroni et al. (2002).

An annular flow model was developed by Qu and Mudawar (2003b) to predict the saturated flow boiling heat transfer coefficient. Laminar liquid and vapor flow, smooth interface, and strong droplet entrainment and deposition effects were incorporated into the model.

Thome et al. (2004) proposed a new heat transfer model for evaporation in the elongated-bubble regime in micro-channels. The model describes the transient variation in local heat transfer coefficient during the sequential and cyclic passage of a liquid slug, an evaporating elongated bubble and a vapor slug. The initial thickness of the liquid film is a key parameter in the model. For this purpose, the Moriyama and Inoue (1996) correlation was used. The main difficulty in implementing the method of Moriyama and Inoue (1996) is in estimating the time for the front of the bubble to reach a particular radius. Thome et al. (2004) developed the expression for film thickness only from R-113 tests. The time averaged local heat transfer coefficient calculated using this model was compared by Dupont et al. (2004) to 1591 experimental data cover tube diameters from 0.77 to 3.1 mm. The data were obtained for the following seven fluids: R-11, R-12, R-113, R-123, R-134a, R-141b, and CO_2. The new model predicts 67% of the database to within ±30%.

An important aspect of flow boiling in micro-channels is the fluctuations of pressure, because these fluctuations can lead to instabilities. Two-phase flow instabilities in parallel boiling channels have been studied both experimentally and theoretically in the past decades for their importance to the safety of boiling heat exchangers. The previous studies of two-phase flow instabilities in parallel boiling channels were carried out on loop that contains channels of conventional size, Kakac and Veziroglu (1983), Kakac et al. (1990). Several types of two-phase flow instabilities were observed: on boiling instability, second density-wave oscillation, density wave oscillation, pressure drop type instability, etc. However, the most common type of dynamic two-phase flow instability encountered in industry is the density wave oscillation, DWO. Wang et al. (1994) investigated DWO oscillations in a single tube. The test section was made of stainless steel tubing of inner diameter 12 mm with the heated length of 3.8 m. Oscillations of mass flux, inlet pressure and wall temperature with periods of 1.5–4.5 s were observed. The oscillation period and amplitude decreased with increase in heat input. The DWO are related to kinematic wave propagation phenomenon. Pressure fluctuations and corresponding temperature oscillations are associated with boiling in micro-channels to a greater extend than in conventional channels. This is because the flow velocities are very low, and bubble formation can cause a significant disruption of low-quality flow. The periodic wetting and rewetting phenomena were observed by Hetsroni et al. (2001, 2002, 2003), Zhang et al. (2002), Steinke and Kandlikar (2003). The explosive vaporization and significant pressure drop fluctuations were observed by Hetsroni et al. (2001, 2002, 2005). Flow pattern, observed in

these studies and reported also by Kandlikar (2002), revealed a flow reversal in some channels with expanding bubbles pushing the liquid–vapor interface in both upstream and downstream directions.

A series of experiments have been carried out by Wu and Cheng (2004) to study boiling instability in eight parallel silicon micro-channels, with trapezoidal cross-section having a hydraulic diameter of 186 μm. Three kinds of unstable boiling modes were observed. Oscillation periods and oscillation amplitudes of temperature, pressure and mass flux measurements were different for the three boiling modes.

Lee et al. (2004a,b) studied experimentally bubble dynamics in a single trapezoid micro-channel and in two parallel micro-channels with a hydraulic diameter of 41.3 μm. Bubble nucleation and growth in parallel micro-channels were observed for some cases with the wall temperature lower than the saturation temperature corresponding to the system pressure. It was reported by Bergles and Kandlikar (2005) that CHF in micro-channels under conditions of low mass flux and low quality may be result of instabilities rather than conventional dryout mechanism.

The main purpose of the present study is to highlight the behavior of pressure drop, wall temperature and heat transfer coefficient under condition of explosive boiling regime, which exists before the annular flow regime. Tests were performed in the range of hydraulic diameter 100–220 μm, mass flux 32–200 kg/m^2 s, heat flux 120–270 kW/m^2, vapor quality $x = 0.01$–0.08.

2. Experimental set-up and procedure

2.1. Experimental facility

The experimental facility and flow loop were described in detail by Hetsroni et al. (2002, 2003). The loop consists of a liquid pump, piping, test module, entrance and exit tanks. Deionized water was used in this study. Working liquid was pumped from the entrance tank through the inlet collector to the micro-channels in the test module, and from the micro-channels through the outlet collector to the exit tank. Tubing of 4.0 mm inner diameter delivered the pumped fluid into the test module and out to the exit tank. The experiments were performed in an open loop, therefore the outlet pressure was close to atmospheric. Two types of pumps were used: peristaltic pump and mini gear pump.

The temperature of the working fluid was measured at the inlet and outlet collectors of the test module, by 0.3 mm type-T thermocouples. The thermocouples were calibrated in 0.1 K increments. The flow rate of the working fluid was measured by weighting method. Pressures were measured at the inlet and the outlet manifolds of the test module by silicon pressure sensors, with sensitivity of 3.3 mV/kPa, response time 1.0 ms. Data were collected by a data acquisition system.

Basic design of the test sections. The test sections, Fig. 1 were fabricated of a square-shape silicon substrate 15×15 mm, 530 μm thick, and utilized a Pyrex cover, 500 μm thick, which served as both an insulator and a transparent cover through which flow in the micro-channels could be observed. The Pyrex cover was

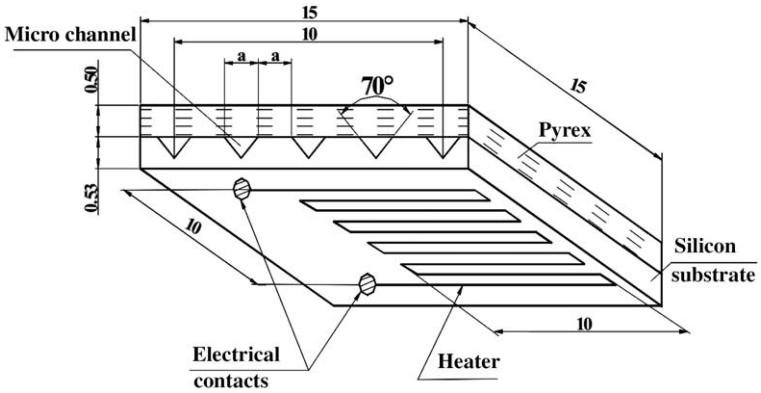

Fig. 1. Test section.

anodically bonded to the silicon chip, in order to seal the channels. In the silicon substrate, parallel micro-channels were etched, the cross-section of each channel was an isosceles triangle. The angles at the base were 55°. We used the test modules having 13, 21, and 26 micro-channels with hydraulic diameters of 220, 130, and 100 μm, respectively. An electrical heater of 10×10 mm^2, made of a thin film resistor, had been deposited on the back surface of the silicon, and served to simulate the heat source. The input voltage and current were controlled by a power supply. The heater was coated with a thin layer of black diffusive paint, with emissivity of $\varepsilon \approx 0.96$. The heater had a serpentine pattern and the heater filament had a dimension of 0.001 mm in thickness, 0.2 mm in width and 250 mm in length. This design allowed a uniform heating of the surface and reduces the contact resistance between the heater and the wafer.

2.2. Flow and thermal visualization

A microscope with zoom ability up to ×40 was connected to an external lighting arrangement. An additional camera joint was assembled to connect a high-speed camera to the microscope. The high-speed camera with maximum frame rate of 10,000 fps, was used to visualize the two-phase flow regimes in the micro-channels. To study the temperature field of the resistor that simulated the heat produced by the electronic transistors, a high-speed Focal Plane Array Radiometer containing 75 kpixels was utilized. The measurement resolution was of 0.03 °C with a standard measurement accuracy of ±2 °C for the range of 0–100 °C and of ±2% above 100 °C. In isolated laboratory environment using an appropriate black body, improved calibration and non-uniformity-correction are possible, therefore an accuracy of ±1 °C can be achieved. Using microscopic lens and reduced array size, IR measurements can be taken at up to 800 Hz with a 30 μm spatial resolution.

2.3. Data reduction

The parameters used in the data reduction and analyses are summarized below:

Heat flux. In order to determine the heat flux from the heater to the working fluid, the heat losses due to conduction, convection and radiation were taken into account. There are several heat transfer surface areas that may be used in the calculations. The first is the plate area of the heater $F = 1 \times 1$ cm^2. The second, F_h, can be defined relative to the mean heat flux along the heated perimeter. A comprehensive discussion on the application of these two definitions to evaluate the mean heat flux is presented by Qu and Mudawar (2003a). In the present study $F = F_h$, and the heat flux transferred to the fluid was defined as

$$q = \varphi N / F_h \tag{1}$$

where φ is the ratio of the heat transferred to the working fluid to the local heat generation, N is the electric power applied to the heater. The procedure of calculating the ratio φ was described by Hetsroni et al. (2005) in great depth. The values of φ estimated with standard deviation of 12% were in the range of 0.8–0.9 depending on flow rate and heat flux.

Mass flux. The mass flux, m, at the inlet of the test section was calculated as

$$m = Q\rho / A \tag{2}$$

where Q is the volumetric flow rate, ρ is the fluid density, and A is the overall cross-section of the micro-channels.

Heat transfer coefficient. The heat transfer coefficient in the boiling regime, assuming thermal equilibrium:

$$h = q/(T_{w,mean} - T_{s,mean}) \tag{3}$$

where h is the heat transfer coefficient, $T_{w,mean}$ is the average temperature at the channel wall where saturated boiling occurs, $T_{s,mean}$ is the average saturation temperature. The pressure at the inlet and the outlet manifolds was measured, and linear interpolation was employed to determine the saturation temperature.

Mass vapor quality at the outlet manifold was calculated from equation of change in the enthalpy of a liquid–vapor system during evaporation in the micro-channels.

Table 1
Experimental uncertainty

No	Source of uncertainty	Symbol	Uncertainty, %
1	Hydraulic diameter	d_h	2
2	Heat flux	q	4
3	Mass flux	m	5
4	Vapor quality	x	12
5	Heat transfer coefficient	h	18
6	Period between events	τ	14
7	Initial film thickness	δ	16

2.4. Experimental uncertainty

The temperature of the heated wall was measured with an accuracy 0.3 K (95% confidence level). The uncertainty of the components for an estimation of an error measurement of wall temperature was obtained according to the standard 1995 Guide to the Expression of Uncertainty of the Measurements (1995 GEUM). The details of calculation are presented by Hetsroni et al. (2005). The error in determining the heat transfer coefficient was calculated from an estimation of the errors that affect the measurements of the following quantities: heat flux and the average temperature difference between heater and the saturation temperature.

The error in determining the power generated by Joule heating is due to errors of measurements of both the electric current and the electric resistance. The error in estimation of the heat losses is due to correlations for calculation of natural convection and radiation heat transfer. The experimental runs were repeated and the average values obtained from the measurements are discussed below. The uncertainties in determining various parameters in this study are given in Table 1.

3. Results

3.1. Dimensionless groups related to periodic explosive boiling

Periodic explosive boiling was studied by Hetsroni et al. (2005) experimentally and a physical model was proposed. However, it was not possible to describe the experimental results by dimensionless groups since the experiments were conducted in micro-channels of one size and for one kind of fluid only. In the present study the experimental determination of the effect of the physical properties, the wall heat flux, the mass flux and the channel size was performed and dimensionless groups proposed based on fundamental considerations.

Fundamental theoretical considerations of the governing forces and their mutual interactions in a heated small size tube are based on our previous study, Hetsroni et al. (2004). It was shown that pressure and temperature oscillations depend on the heat flux, mass flux (or flow velocity in the channels), physical liquid properties and channel size. For flow boiling heat transfer the Nusselt number $Nu = hd/k$ is widely used, where d is the characteristic dimension, h is the heat transfer coefficient, k is the thermal conductivity of the liquid (see Tables 2–5).

According to Yao and Chang (1983) boiling in a confined space is mainly characterized by the deformation of the bubbles. They reported that the bubble deformation can be characterized by the ratio of the gap size and the nominal bubble departure diameter, which is generally known as Bond or Eotvos number. As proposed by Kew and Cornwell (1997), the Eotvos number may be used to take into consideration confinement on boiling.

It is well known that at high enough mass fluxes, Eotvos number, $Eo = g(\rho_L - \rho_G)d^2/\sigma$ (where g is the acceleration due to gravity, ρ_L and ρ_G are the liquid and vapor density, respectively, d is the characteristic dimension, σ is the surface tension) is not expected to play an important role in micro-channels, since the effect of gravitational force is small except at very low mass fluxes and vapor fractions. The distinctive property of the present experiments is very low values of mass fluxes and vapor qualities and Eo should be introduced in heat transfer correlations. The combined effect of heat flux and mass flux appears only in the boiling number, $Bo = q/mh_{LG}$, where q is the heat flux, m is the mass flux, h_{LG} is the latent heat of vaporization. We used these dimensionless groups to describe heat transfer phenomenon. We proposed that heat from the wall was

Table 2
Water boiling. Hydraulic parameters in an individual micro-channel in the test module

Number of micro-channels n	Hydraulic diameter d_h (mm)	Mass flux m (kg/m^2 s)	Heat flux q (kW/m^2)	Fluid velocity U (m/s)	Period between events τ (s)	Initial film thickness δ (μm)	Reynolds number Re	Boiling number Bo	Dimensionless period τ^*	Dimensionless thickness δ^*
13	0.22	31.6	105	0.032	0.14	6.6	23	0.00147	21	0.71
		31.6	139	0.032	0.10	6.3	23	0.00194	15	0.68
		63.3	166	0.063	0.062	4.5	46	0.00116	18	0.95
		63.3	197	0.063	0.035	3.0	46	0.00138	10	0.64
21	0.13	95.0	176	0.095	0.05	3.8	41	0.000819	37	1.2
		95.0	201	0.095	0.038	3.3	41	0.000936	28	1.1
		95.0	269	0.095	0.031	3.6	41	0.00125	23	1.2
		95.0	124	0.095	0.15	7.8	41	0.000577	107	2.5
		95.0	131	0.095	0.11	6.5	41	0.000610	84	2.1
		95.0	132	0.095	0.13	7.4	41	0.000615	94	2.4
		95.0	141	0.095	0.12	7.2	41	0.000657	86	2.3
		95.0	147	0.095	0.071	4.5	41	0.000684	52	1.5
		95.0	158	0.095	0.091	6.3	41	0.000736	67	2.0
		95.0	175	0.095	0.044	3.4	41	0.000815	32	1.1
		95.0	179	0.095	0.056	4.4	41	0.000833	41	1.4
		95.0	190	0.095	0.042	3.5	41	0.000885	31	1.1
		95.0	193	0.095	0.047	3.9	41	0.000899	35	1.3
		95.0	213	0.095	0.04	3.7	41	0.000992	30	1.2
		95.0	228	0.095	0.028	2.8	41	0.00106	21	0.89
		95.0	270	0.095	0.022	2.6	41	0.00126	16	0.83
26	0.10	68.1	148	0.067	0.076	4.9	23	0.000961	49	1.1
		68.1	159	0.067	0.065	4.5	23	0.00103	42	1.0
		135	163	0.135	0.065	4.6	47	0.000535	85	2.1
		135	190	0.135	0.046	3.8	47	0.000623	60	1.7
		135	221	0.135	0.034	3.3	47	0.000725	45	1.5
		203	254	0.203	0.032	3.5	71	0.000554	63	2.4

Table 3
Boiling of ethanol. Hydraulic parameters in individual micro-channel in the test module

Number of micro-channels n	Hydraulic diameter d_h (mm)	Mass flux m (kg/m^2 s)	Heat flux q (kW/m^2)	Fluid velocity U (m/s)	Period between events τ (s)	Initial film thickness δ (μm)	Reynolds number Re	Boiling number Bo	Dimensionless period τ^*	Dimensionless thickness δ^*
13	0.22	60.8	67.0	0.063	0.060	5.2	17	0.00114	17	0.54
		60.8	85.0	0.063	0.045	5.0	17	0.00145	13	0.51
		60.8	108	0.063	0.039	5.5	17	0.00185	11	0.56
		60.8	118	0.063	0.030	4.6	17	0.00202	8.5	0.48

removed by periodic liquid film motion induced by vapor bubbles rising in the micro-channel and by periodic dry out due bubbles venting. Thus we related the Nusselt number to boiling and Eotvos numbers, which characteristic length being the hydraulic diameter of the micro-channel. As such, we correlated the data as

$$Nu \sim C_1 Bo^{m1} Eo^{n1} \tag{4}$$

The exponent m_1, and n_1, and the proportionality constant C_1, were found empirically.

In the present study we investigated a new type of instability that took place in an individual channel of the heat sink that contains a number of parallel micro-channels: oscillations due to the explosive nature of the boiling: explosive boiling oscillations, EBO. The main parameter effects on EBO in an individual channel of the heat sink such as hydraulic diameter, mass flux, heat flux were studied. The goal of the present study was also to connect the heat transfer with flow instabilities. The theoretical analysis performed by Hetsroni

Table 4
Water boiling. Heat transfer related to whole heated surface of the module that contains parallel micro-channels

Number of micro-channels n	Hydraulic diameter d_h (mm)	Mass flux m (kg/m^2 s)	Heat flux q (kW/m^2)	Fluid velocity U (m/s)	Heat transfer coef. h (W/m^{2}K)	Reynolds number Re	Boiling number Bo	Nusselt number Nu	Eotvos number Eo	ONB L_{ONB} (mm)
13	0.22	31.6	105	0.032	10,000	23	0.00147	3.3	0.00801	5.1
		31.6	139	0.032	1100	23	0.00194	3.5	0.00801	3.9
		63.3	166	0.063	14,000	46	0.00116	4.7	0.00801	6.5
		63.3	197	0.063	13,000	46	0.00138	4.3	0.00801	5.5
		94.9	214	0.095	21,000	70	0.000998	6.8	0.00801	7.5
		94.9	246	0.095	18,000	70	0.00115	5.7	0.00801	6.6
		127	266	0.13	27,000	93	0.000930	8.7	0.00801	8.1
		1267	291	0.13	22,000	93	0.00102	7.0	0.00801	7.4
21	0.13	95.0	159	0.095	17,000	42	0.000740	3.3	0.00281	6.1
		95.0	217	0.095	13,000	42	0.00101	2.5	0.00281	4.4
		143	214	0.14	26,000	62	0.000664	4.9	0.00281	6.8
		143	251	0.14	15,000	62	0.000779	2.9	0.00281	5.8
		190	244	0.19	35,000	83	0.000568	6.6	0.00281	7.9
		190	290	0.19	29,000	83	0.000675	5.5	0.00281	6.7
		238	331	0.24	26,000	104	0.000616	5.0	0.00281	7.3
26	0.10	68.1	144	0.067	8300	23	0.000935	1.2	0.00166	3.8
		135	190	0.14	19,000	47	0.000623	2.9	0.00166	5.8
		135	217	0.14	15,000	47	0.000712	2.3	0.00166	5.0
		135	217	0.14	13,000	47	0.000712	1.9	0.00166	5.0
		203	274	0.20	17,000	71	0.000597	2.5	0.00166	6.0
		270	325	0.27	23,000	94	0.000533	3.4	0.00166	6.7
		338	365	0.34	31,000	118	0.000478	4.6	0.00166	7.5

Table 5
Boiling of ethanol. Heat transfer related to whole heated surface of the module that contains parallel micro-channels

Number of micro-channels n	Hydraulic diameter d_h (mm)	Mass flux m (kg/m^{2}s)	Heat flux q (kW/m^2)	Fluid velocity U (m/s)	Heat transfer coefficient h (W/m^{2}K)	Reynolds number Re	Boiling number Bo	Nusselt number Nu	Eotvos number Eo	ONB L_{ONB} (mm)
13	0.22	28.5	50.7	0.032	4900	8.6	0.00184	6.3	0.0219	4.1
		28.5	62.9	0.032	4600	8.6	0.00229	6.0	0.0219	3.3
		28.5	73.2	0.032	4100	8.6	0.00266	5.3	0.0219	2.8
		60.8	84.9	0.063	7900	17	0.00145	10	0.0219	5.2
		60.8	108	0.063	8100	17	0.00184	10	0.0219	4.2
		60.8	112	0.063	6200	17	0.00192	8.0	0.0219	3.9
		93.1	105	0.095	9800	26	0.00117	13	0.0219	6.4
		93.1	126	0.095	9400	26	0.00141	12	0.0219	5.3
		93.1	150	0.095	9300	26	0.00168	12	0.0219	4.5
		124	138	0.13	10,000	34	0.00115	13	0.0219	6.5
		124	162	0.13	9400	34	0.00135	12	0.0219	5.6

et al. (2004) and experimental results reported by Hetsroni et al. (2005) showed that the period of successive periodic cycles, τ, depends on the heat and mass fluxes. Thus we used the dimensionless groups $\tau^* = \tau/Ud$ and boiling number Bo. The dependence of dimensionless time on boiling number can be assumed as

$$\tau^* \sim C_2 Bo^{m2} \tag{5}$$

Correlations (4) and (5) describe experimental results adequately. However, because of the complex nature of the sub processes involved, it has not been possible to develop comprehensive correlations for these parameters.

3.2. Quasi-periodic boiling in a certain single micro-channel of heat sink

In the present study we investigated a new type of instability that took place in an individual channel of a heat sink that contains a number of parallel micro-channels: explosive boiling oscillations, EBO. The main parameters that effect the EBO in an individual channel of the heat sink such as hydraulic diameter, mass flux, heat flux were studied. During EBO the pressure drop oscillations were always accompanied by wall temperature oscillations. However, in contrast to DWO, the period of these oscillations was very short and the oscillation amplitude increased with an increase in heat input. This type of oscillations was found to occur at low vapor quality.

Flow visualization. The analysis is based on a previous explosive boiling model suggested by Hetsroni et al. (2005). Flow boiling in parallel channels was studied from the subcooled liquid entry, at the inlet, to a liquid–vapor mixture flow at the outlet. Once the nucleation begins, the heat flux causes a sudden release of energy into the vapor bubble, which grows rapidly and occupies the entire channel. The vapor slug may be considered as an elongated bubble. The rapid bubble growth pushes the liquid–vapor interface on both caps of the vapor slug at the upstream and the downstream ends and leads to a reversed flow. When in some parallel channels the liquid on the upstream side is pushed back, the other parallel channels carry the resulting excess flow. The behavior of the long vapor bubbles occurring in a micro-channel was not similar to annular flow with intermitted slugs of liquid between two long vapor trains. The periodic phenomenon described above may be regarded as explosive boiling. The trigger mechanism of such a regime is venting of elongated bubble due to very rapid expansion.

The following regimes were observed: regime of alternated liquid–vapor flow before venting of elongated bubble. It is located upstream of the ONB point. Fig. 2 shows the unsteady flow, upstream of the ONB in

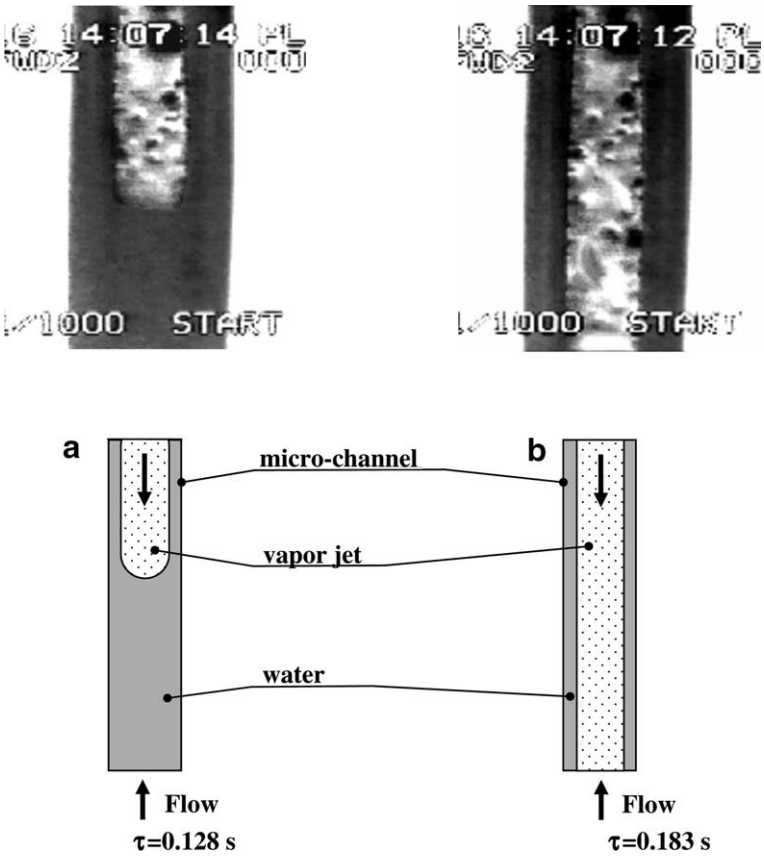

Fig. 2. Flow pattern upstream the ONB: (a) single phase water flow, (b) jet that penetrate the bulk of the water.

one of the parallel micro-channels of d_h=130 μm at $q = 228$ kW/m^2, $m = 0.044$ g/s. In this part of the micro-channel the single phase water flow was mainly observed. Clusters of water appeared as a jet, penetrating the bulk of the water, Fig. 2a. The vapor jet moved in the upstream direction, and the space that it occupied increased, Fig. 2b. In Fig. 2a and b the flow moved from bottom to top. These pictures were obtained at the same part of the micro-channel but not simultaneously. The time interval between events shown in Fig. 2a and b is 0.055 s. As a result, the vapor was accumulated in the inlet plenum. The second regime may be attributed to the venting of the elongated bubble and evaporating of liquid film from the heated channel wall. This regime is located downstream of the ONB point and is characterized by a period t. Fig. 3 shows the regime downstream of the ONB. Hot spots (dryout) were observed, Fig. 3a. The temperature of the heated wall did not increase sharply, as in the CHF case, due to periodical nature of the process. After a certain time the micro-channel was again supplied with liquid, Fig. 3b. The mass flux and channel hydraulic diameter affect the ONB location. The general trend of heat flux on the location of the ONB is similar to that in ordinary sized channel, i.e., at a given flow rate the ONB location generally moves upstream, as the heat flux is increased.

Period between successive events. Fig. 4 shows the dependence of the dimensionless period of phase transformations (i.e. the time between bubble venting), τ^*, on boiling number, Bo, ($\tau^* = \tau/Ud_h$, $Bo = q/mh_{LG}$, τ is the period between successive events, U is the mean velocity of single phase flow in the micro-channel, d_h is the hydraulic diameter of the channel, q is heat flux, m is mass flux, h_{LG} is the latent heat of vaporization). The dependence τ^* on Bo can be approximated, with standard deviation of 16%, by

$$\tau^* = 0.000030Bo^{-2} \tag{6}$$

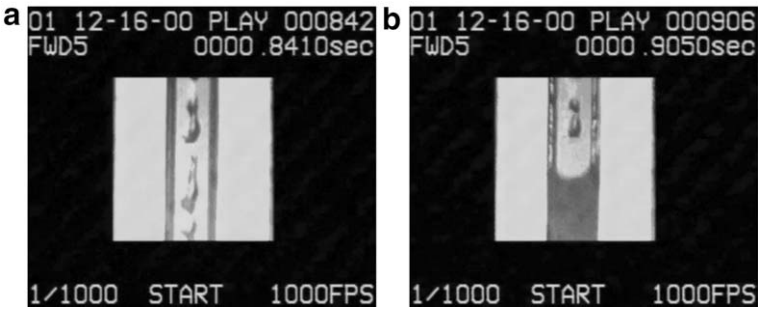

Fig. 3. Flow pattern downstream the ONB: (a) dryout, (b) single phase water flow.

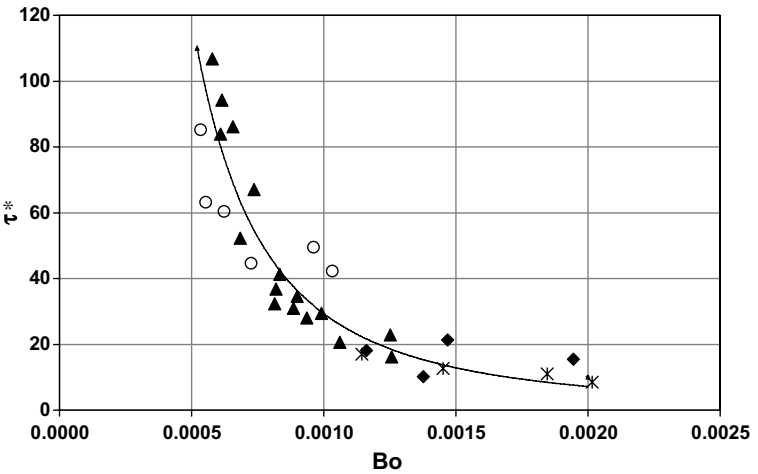

Fig. 4. Dependence of dimensionless time interval between cycles on boiling number: ○ $D_h = 100$ μm, water, ▲ $D_h = 130$ μm, water, ♦ $D_h = 220$ μm, water, ✳ $D_h = 220$ μm, ethanol.

The initial thickness of the liquid film. The evaporation of the liquid layer on the wall was employed by Qu and Mudawar (2003b) and Thome et al. (2004) to predict the heat transfer coefficient. In the present study the term initial liquid film thickness is defined as the average thickness of fluid, evenly distributed during period t, over the surface of the circular micro-channel, after venting of the elongated bubble. This surface is located downstream of the ONB and may be characterized by the heated length, L, and hydraulic diameter, d_h. We assumed that during the period, t, the liquid film has disappeared due to evaporation. The heat removed from the wall surface is the same as required for the liquid film evaporation during the period, t. The heat balance is

$$\pi\delta d_h L\rho_L = q\pi d_h L t/h_{LG} \tag{7}$$

where ρ_L is the liquid density.

The average liquid thickness, δ, can be calculated as

$$\delta = qt/\rho_L h_{LG} \tag{8}$$

Fig. 5 shows dependence of the dimensionless initial liquid thickness of water and ethanol, δ^*, on the boiling number, Bo, where $\delta^* = \delta U/v$, U is the mean velocity of single phase flow in the micro-channel, v is the kinematic viscosity of the liquid at saturation temperature. The dependence of δ^* on Bo can be approximated, with standard deviation of 18%, by

$$\delta^* = 0.00015Bo^{-1.3} \tag{9}$$

The initial thickness of the liquid film is a key parameter of the explosive boiling. This point may be discussed in some detail with regard to the beginning of the critical heat flux, CHF, regime. The variation of the initial thickness of the film of water vs. the heat flux is provided in Fig. 6. For explosive boiling the film thickness decreases with increasing heat flux from 125 to 270 kW/m^2 from about 8 μm to 3 μm. This range of values is of the same order of magnitude as those given by Moriyama and Inoue (1996) and by Thome et al. (2004) for R-113 in small spaces (100–400 μm). Decreasing liquid film thickness with increasing heat flux is a distinct feature of dryout during explosive boiling. Under these conditions at which the instantaneous temperature of the heater surface exceeds 125 °C, the value of δ was in the range of 3 ± 0.6 μm. This value may be considered as minimum initial film thickness. If the liquid film reached the minimum initial film thickness, δ_{min}, CHF regime occurred. According to Thome et al. (2004) δ_{min} is assumed to be on the same order of magnitude as the surface roughness. The values of the minimum initial film thickness calculated by Thome et al. (2004) for R-113 at saturation temperature 47.2 °C was in the range of 1.5–3.5 μm.

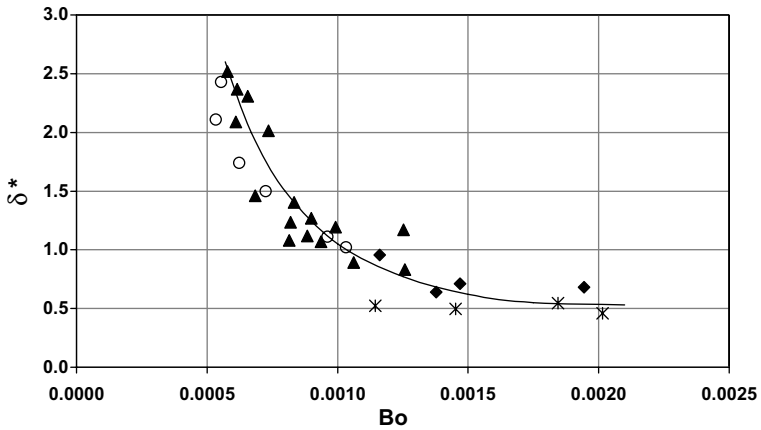

Fig. 5. Dependence of dimensionless initial film thickness on boiling number: ○ $D_h = 100$ μm, water, ▲ $D_h = 130$ μm, water, ♦ $D_h = 220$ μm, water, ✳ $D_h = 220$ μm, ethanol.

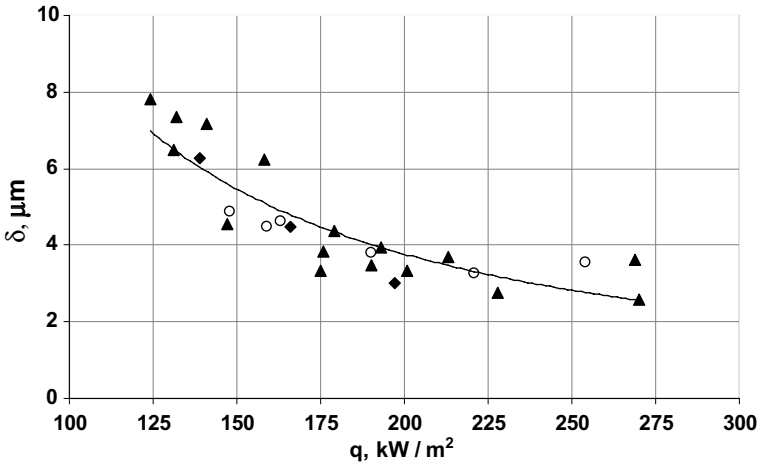

Fig. 6. Variation of initial film thickness for water versus heat flux: ○ $D_h = 100$ μm, water, ▲ $D_h = 130$ μm, water, ◆ $D_h = 220$ μm, water.

3.3. System that contain a number of parallel micro-channels

We studied also the effect of EBO in individual channels on average characteristics of the whole heat sink: total pressure drop and temperature fluctuations on the heater, and heat transfer coefficient. The high frequency oscillations in individual micro-channels are superimposed and lead to total low frequency pressure drop and temperature oscillations of the system.

Fluctuation of pressure drop, fluid and heated wall temperatures. In this study, we have carried out experimental investigations on boiling instability in parallel micro-channels by simultaneous measurements of temporal variations of pressure drop, fluid and heater temperatures. The channel-to-channel interactions may affect pressure drop between the inlet and the outlet manifold as well as associated temperature of the fluid in the outlet manifold and heater temperature. Fig. 7 illustrates this phenomenon for pressure drop in the heat sink that contains 13 micro-channels of $d_h = 220$ μm at mass flux $m = 93.3$ kg/m^2 s and heat flux $q = 200$ kW/m^2. The temporal behavior of the pressure drop in the whole boiling system is shown in Fig. 7a. The considerable oscillations were caused by the flow pattern alternation, that is, by the liquid/two-phase alternating flow in the micro-channels. The pressure drop FFT is presented in Fig. 7b. Under condition of the given experiment the period of pressure drop fluctuation is about $\tau = 0.36$ s. The results differ significantly from those reported by Wu and Cheng (2004). In the range of average values of mass flux $m = 112$–146 kg/m^2 s and heat flux $q = 135$–226 kW/m^2 the authors observed much longer oscillation period (from $\tau = 15.4$ to 202 s). In experiments conducted by Wu and Cheng (2004), the water in the pressure tank was moved by the compressed nitrogen gas to the test section. According to the authors when the boiling occurred in the test section, the pressure drop across the test was suddenly increased due to generation of vapor bubbles. This increase in pressure drop caused a decrease in mass flux. The long period pressure drop fluctuations may be connected to the period of increasing or decreasing of incoming mass flux. The former depends not only on boiling in the micro-channels of heat sinks, but also on the nitrogen pressure in the water tank and the total length of the pipe connecting the water tank to the test section. In our experiments, the mass flow rate was independent of pressure drop fluctuations, and the oscillation periods are very much different from those recorded by Wu and Cheng (2004).

The pressure drop fluctuation provides insight into the temperature behavior of the fluid in the outlet manifold. The pressure drop fluctuation frequency is representative for the oscillations in the system. Fig. 8a and b shows time variation and FFT of fluctuation component of the fluid temperature, respectively. From Fig. 8a one can see that the average fluid temperature at the outlet manifold is less than the saturation temperature. These results in the fact that only single liquid comes to the outlet manifold through some of the parallel micro-channels.

The time variation of the mean and maximum heater temperature is presented in Fig. 9. The mean heater temperature (i.e. the average temperature of the whole heater) changed in the range of $\Delta T_{av} = 10$ K. The

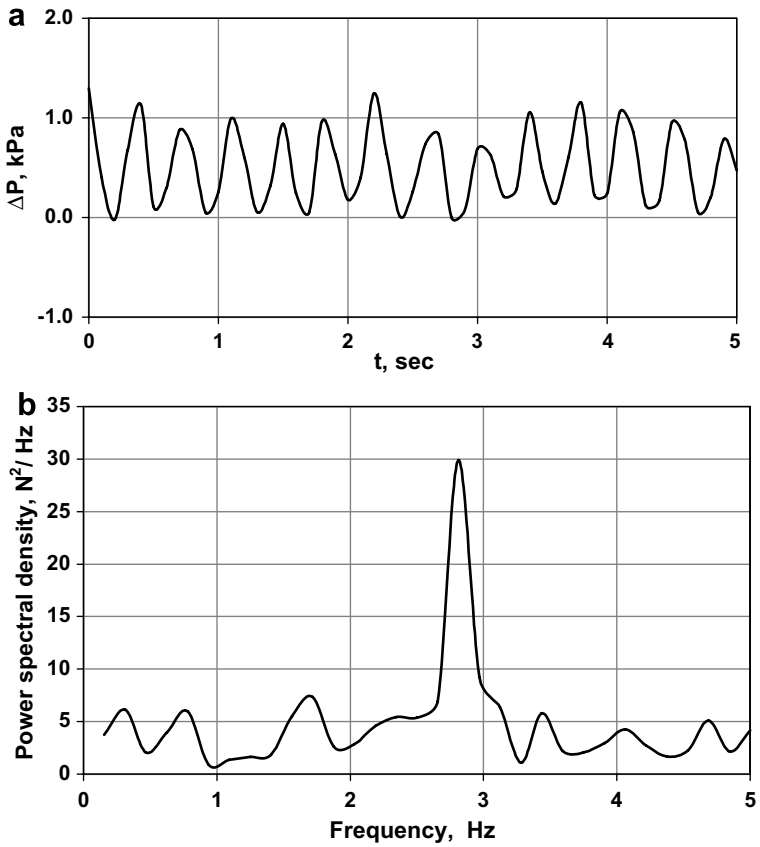

Fig. 7. Time variation of pressure drop at $q = 200\ \mathrm{kW}/m^2$: (a) pressure drop fluctuations, (b) pressure drop amplitude spectrum.

maximum heater temperature changed in the range of $\Delta T_{\max} = 6$ K. Comparison between Figs. 7–9 shows that the time period (frequency) is the same for the pressure drop, the fluid temperature at the outlet manifold, the mean and maximum heater temperature fluctuations. It also allows one to conclude that these fluctuations are in phase.

When the heat flux is increased, at constant value of mass flux, the oscillation amplitudes of the pressure drop, the fluid and the heater temperatures also increase. Figs. 10–12 show temporal variations of the pressure drop and temperatures at mass flux $m = 93.3\ \mathrm{kg/m^2\ s}$ and heat flux $q = 220\ \mathrm{kW/m^2}$. From Fig. 12 one can see that the average heater temperature changed in the range of $\Delta T_{\mathrm{av}} = 13$ K. The maximum heater temperature changed in the range of $\Delta T_{\max} = 10$ K.

When the heat flux was further increased to $q = 260\ \mathrm{kW/m^2}$ the liquid-phase period did not disappear and the continuous two-phase flow was not observed throughout the parallel micro-channels. The behavior of the heater temperatures is shown in Fig. 13. The average values of the whole and maximum heater temperatures are about $T_{\mathrm{mean}} = 110\ ^\circ\mathrm{C}$ and $T_{\max} = 120\ ^\circ\mathrm{C}$. The maximum heater temperature varied in the range of $\Delta T_{\max} = 20$ K (i.e. from 110 °C to about 130 °C). This is somewhat unexpected. While numerous types of flow patterns observations in micro-channel flow were reported in the literature, this issue has received very limited attention, despite its importance for the design and safe operation of a heat sink. CHF generally refers to a sudden decrease in the heat transfer coefficient for a surface on which boiling is occurring. For a heat flux-controlled system exceeding CHF can lead to a sudden increase in the average surface temperature. Under conditions discussed above ($m = 93.3\ \mathrm{kg/m^2\ s}$ and heat flux $q = 260\ \mathrm{kW/m^2}$) the average temperature of the whole heater was about $T_{\mathrm{mean}} = 110\ ^\circ\mathrm{C}$, whereas the maximum temperature reaches periodically the value of 130 °C, which for most heat sinks can lead to catastrophic system failure. The ability to determine instan-

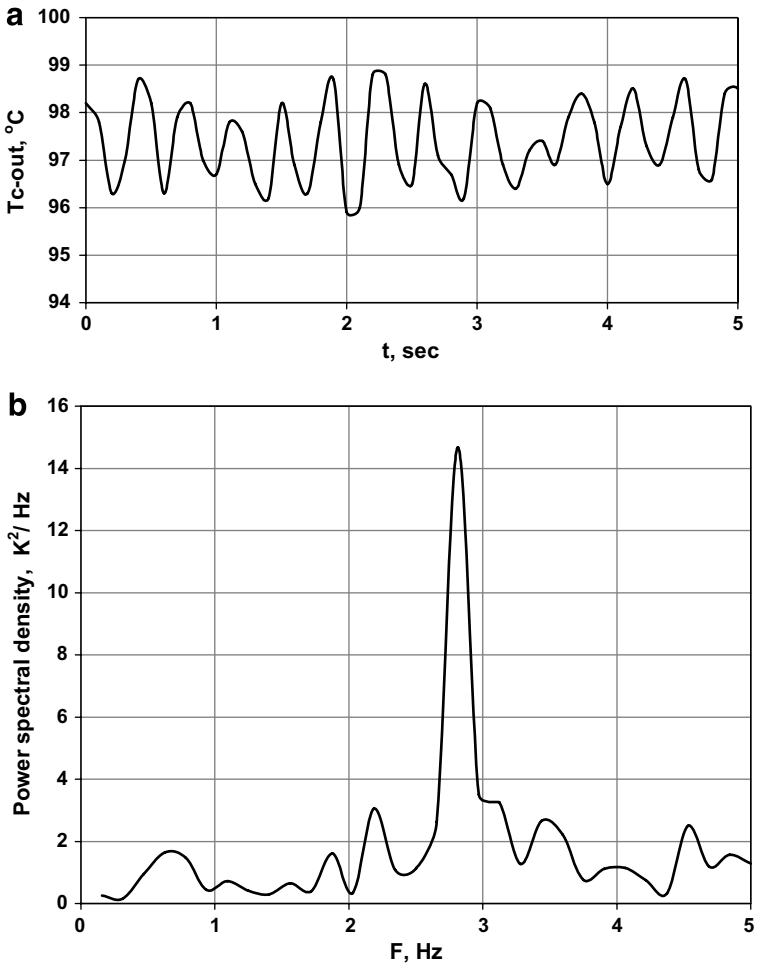

Fig. 8. Time variation of fluid temperature at the outlet manifold, $q = 200\ \mathrm{kW/m^2}$: (a) temperature fluctuations, (b) temperature amplitude spectrum.

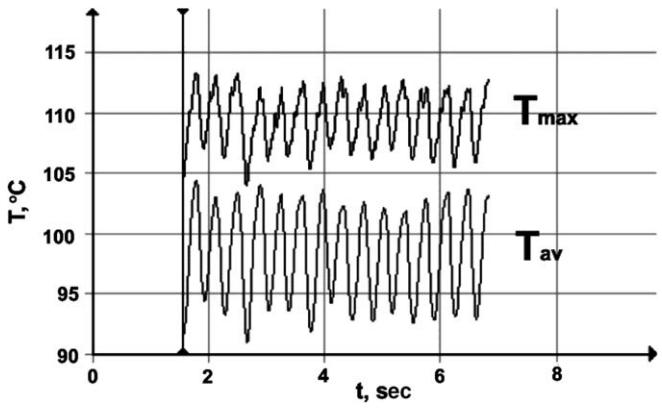

Fig. 9. Time variation of average and maximum heater temperature at $q = 200\ \mathrm{kW/m^2}$.

taneous maximum of surface temperature is of vital importance to the safety of two-phase micro-channel heat sink. From Figs. 10–12 one can conclude that periods of oscillations increased with increasing power. Such a

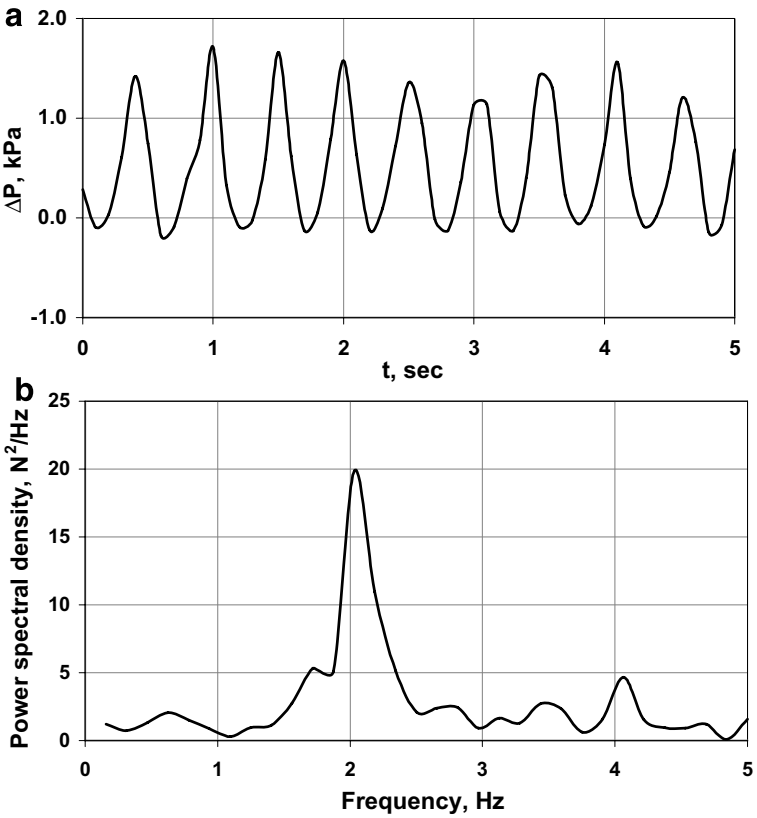

Fig. 10. Time variation of pressure drop at $q = 20\ \mathrm{kW/m^2}$: (a) pressure drop fluctuations, (b) pressure drop amplitude spectrum.

behavior is quite different from that observed during DWO in a channel of conventional size. Dryout should be taken into account to develop a model of instability during explosive boiling in micro-channels.

3.4. Average heat transfer coefficient

The effect of the boiling number. Fig. 14 shows the dependence of the average heat transfer coefficient, h, on the boiling number, $Bo = q/mh_{\mathrm{LG}}$, for water and ethanol in micro-channels. As indicated in Fig. 14 the heat transfer coefficient decreases appreciably with increasing Bo. These results are in contradiction with those reported by Kandlikar and Balasubramanian (2004), Kandlikar (2004), Steinke and Kandlikar (2004). The authors demonstrated that the general Kandlikar (1990) correlation can be modified to give good agreement with micro-channel flow. Only the nucleate boiling dominant portion of the flow boiling equation suggested by Kandlikar (1990) was used to predict heat transfer coefficient. According this equation $h \sim Bo^{0.7}$. The optimal range of the correlation is between vapor qualities of 0.2–0.8. The correlation under predicts the heat transfer coefficients at low qualities near the ONB condition. This is expected since the rapid bubble growth that we observed in the present study led to periodic local dryout.

Local dryout condition. Dryout occurs when the initial liquid film is not evenly distributed over the heated surface and during rapid evaporation of the liquid film. The results of the flow visualization were reported previously by Hetsroni et al. (2005). The initial liquid film thickness decreases with an increase in the heat flux. The local surface temperatures rise, as there is no film on the surface. As it was shown above, the temporal behavior of the pressure drop leads to fluctuations of the surface temperature of the heater. An increase in the heat flux, at constant mass flux, or decrease in mass flux at constant heat flux, i.e. increase in boiling number, shifts the onset of dryout toward the inlet. This causes the decrease in heat transfer coefficient. The CHF phenomenon is different from that observed in a single channel of conventional size. A key differ-

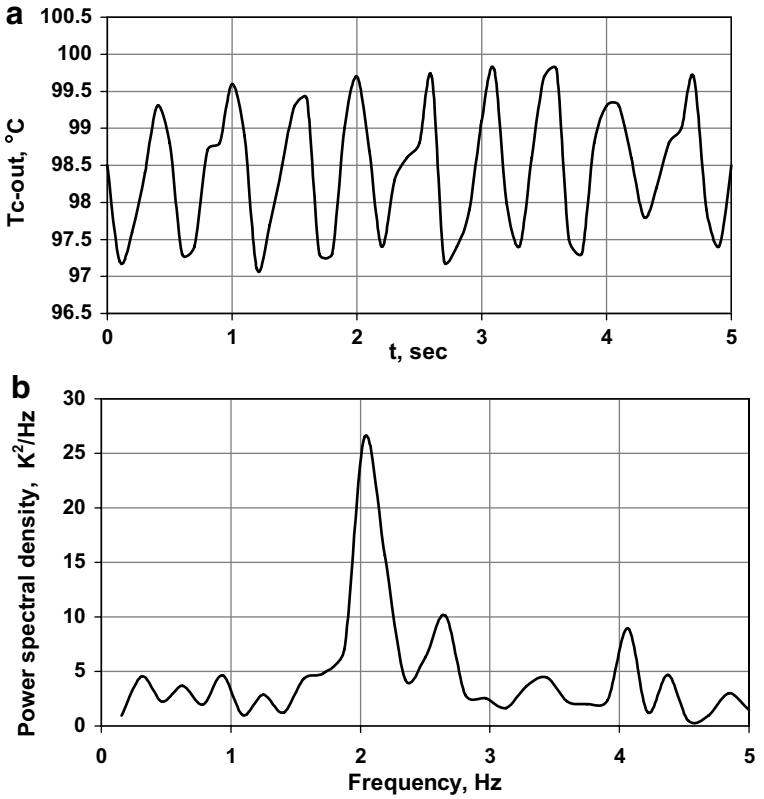

Fig. 11. Time variation of fluid temperature at the outlet manifold, $q = 220\ \mathrm{kW/m^2}$: (a) temperature fluctuations, (b) temperature amplitude spectrum.

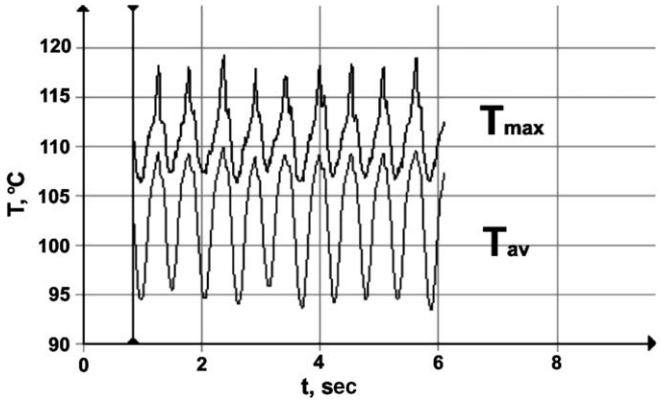

Fig. 12. Time variation of average and maximum heater temperature at $q = 220\ \mathrm{kW/m^2}$.

ence between micro-channel heat sink and single conventional channel is amplification of parallel-channel instability prior to CHF. This amplification causes back flow of vapor into the upstream plenum, which results in an increase of the heated surface temperature. As the heat flux approached CHF, the parallel-channel instability, which was moderate over a wide range of heat fluxes, became quite intense and should be associated with maximum temperature fluctuation of the heated surface. During water boiling the test module, which contains 13 parallel micro-channels of $d_h = 220\ \mu\mathrm{m}$, the temperature fluctuation on the heater are presented in Table 6. At boiling numbers $Bo = 0.0010$–0.0015 the variation of the heater temperature due to instabilities

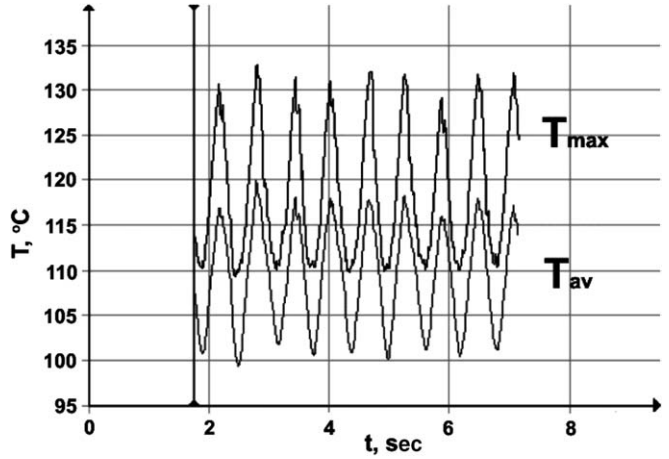

Fig. 13. Time variation of average and maximum heater temperature at $q = 220\ \mathrm{kW/m^2}$.

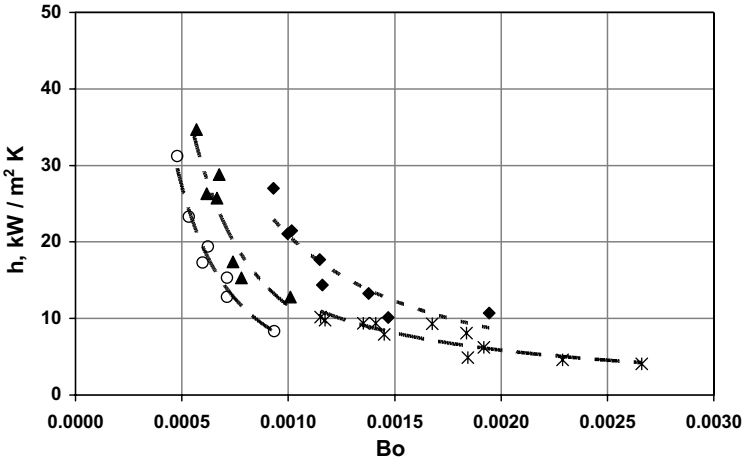

Fig. 14. Dependence of average heat transfer coefficient on boiling number: ○ $D_h = 100\ \mu m$, water, ▲ $D_h = 130\ \mu m$, water, ◆ $D_h = 220\ \mu m$, water, ✳ $D_h = 220\ \mu m$, ethanol.

Table 6
Wall temperature and pressure drop fluctuations of the system that contains 13 parallel micro-channels of $d_h = 220\ \mu m$

Mass flux m (Kg/m^2 s)	Heat flux q (kW/m^2)	Boiling number Bo	Fluctuation frequency f (Hz)	Range of max wall temperature fluctuations $(T_w)_{max} - (T_w)_{min}$ (K)	Range of max pressure drop fluctuations $(\Delta P)_{max} - (\Delta P)_{min}$
63.3	170	0.012	1.6	6.0	2.0
63.3	200	0.014	1.4	23.0	3.5
93.3	200	0.00095	2.8	6.0	1.0
93.3	220	0.001	2.1	10.0	1.6
93.3	260	0.0012	1.9	20.0	2.2
127	260	0.00091	2.4	6.0	1.0
127	320	0.0012	2.2	22.0	2.0

were in the range of $((T_W)_{max} - (T_W)_{min}) = 20$–$23$ K, and the maximum heater temperature exceeded 130 °C. This variation preceded CHF.

Effect of the physical properties of the fluid. Comparison between dependence of the heat transfer coefficients on boiling number, which was obtained in micro-channels of $d_h = 220$ μm for boiling of water and ethanol, shows that the results are different, as expected. In reality, the effects will depend on the fluid properties. At boiling number $Bo = 1.16 \times 10^{-3}$ the heat transfer coefficient is about $h = 15000$ W/m^2 K for water. At about the same boiling number $Bo = 1.14 \times 10^{-3}$ the heat transfer coefficient is about $h = 10000$ W/m^2 K for ethanol, Fig. 14. Boiling number represents such fluid property as the heat of vaporization. One may conclude that the surface tension also affects heat transfer. In a recent publication Kandlikar (2004) presented two new non-dimensional groups that are thought to be important in micro-channel flows. These groups include the surface tension and hydraulic diameter.

The effect of the hydraulic diameter. Fig. 14 shows that for the same value of the boiling number the heat transfer coefficient increases with an increase in the hydraulic diameter. For example, for boiling number of about $Bo = 0.8 \times 10^{-3}$, the heat transfer coefficients were about $h = 9000$, 12,000, and 22,000 W/m^2 K for $d_h = 100$, 130, and 220 μm, respectively. For pipe flow the length of single phase flow from the inlet to ONB for two different diameters d_1 and d_2 may be estimated as

$$m_1 \pi d_1^2 C_p (T_s - T_{in})/4 = q_1 \pi d_1 L_{(ONB)1} \tag{10}$$

$$m_2 \pi d_2^2 C_p (T_s - T_{in})/4 = q_2 \pi d_2 L_{(ONB)2} \tag{11}$$

where m_1 and m_2 is the mass flux, C_p is the specific heat, T_s is the saturation temperature, T_{in} is the inlet temperature, q_1 and q_2 is the heat flux, $L_{(ONB)1}$ and $L_{(ONB)2}$ is the distance from the inlet to ONB point.

From (5) and (6) one can obtain (when T_s and T_{in} do not change)

$$Bo_2 d_1 / Bo_1 d_2 L_{(ONB)1} / L_{(ONB)2} \tag{12}$$

Assuming $Bo_2 = Bo_1$

$$d_1/d_2 = L_{(ONB)1}/L_{(ONB)2} \tag{13}$$

At the same boiling number and inlet temperature, an increase in diameter shifts the ONB farther from the inlet. The region of the local dryout decreases and the average heated surface temperature decreases as well. Under this condition the heat transfer coefficient increases with increased hydraulic diameter. In order to take into account the effect of surface tension and micro-channel hydraulic diameter, we have applied Eotvos number $Eo = g(\rho_L - \rho_G) d_h^2/\sigma$. Fig. 15 shows the dependence of the Nu/Eo on the boiling number, Bo, where $Nu = h d_h/k_L$ is the Nusselt number, h is the heat transfer coefficient, k_L is the thermal conductivity of fluid. All fluid properties are taken at saturation temperature. This dependence can be approximated, with standard deviation of 18%, by relation

$$Nu/Eo = 0.030 Bo^{-1.5} \tag{14}$$

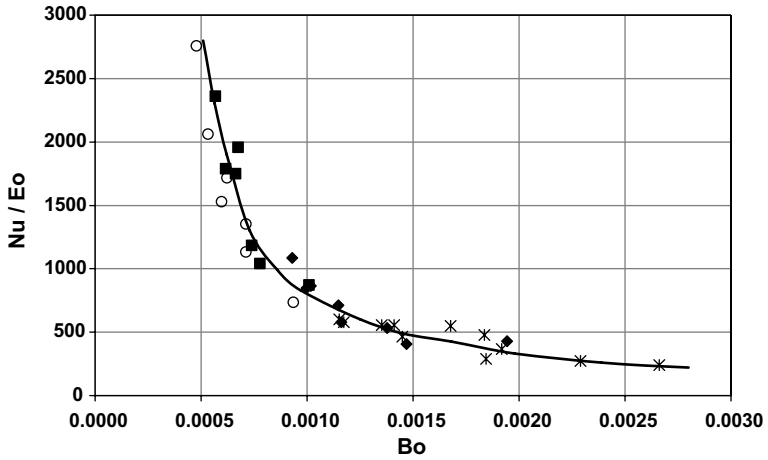

Fig. 15. Dependence of Nu/Eo on Bo. ○ $D_h = 100$ μm, water, ▲ $D_h = 130$ μm, water, ◆ $D_h = 220$ μm, water, ✳ $D_h = 220$ μm, ethanol.

The experimental results obtained in the present investigation can be used in next studies to propose a model of system instability to predict the influences of the geometry, connection between micro-channels, and connection between micro-channels and external loop.

4. Conclusions

The flow visualization showed that the heat flux causes a sudden release of energy into the vapor bubble, which grows rapidly and occupies the entire channel. The rapid bubble growth pushes the liquid–vapor interface on both caps of the vapor bubble, at the upstream and the downstream ends, and leads to a reverse flow. This phenomenon may be regarded to explosive boiling. The trigger mechanism of such a regime is venting of elongated bubble due to very rapid expansion.

The dimensionless period between successive events, $\tau^* = \tau/Ud_h$, depends on boiling number, $Bo = q/mh_{LG}$, and decreases with an increase in the boiling number. The initial thickness of the liquid film is a key parameter of explosive boiling. For explosive boiling of water and ethanol, the film thickness decreases with increasing the heat flux. When the liquid film reached the minimum initial film thickness, δ_{min}, CHF regime occurred. The minimum initial film thickness was assumed to be on the same order of magnitude as the surface roughness. Dimensionless initial film thickness and parameter Nu/Eo depend on the boiling number, i.e. boiling number may be used to connect hydrodynamic and heat transfer phenomena.

Simultaneous measurements of temporal variations of pressure drop, fluid and heater temperatures show the boiling instability in parallel micro-channels. The channel-to-channel interactions may affect pressure drop between the inlet and the outlet manifold, as well as associated temperature of the fluid in the outlet manifold and the temperature of the heater. The frequency is the same for the pressure drop, the fluid temperature at the outlet manifold, and for the fluctuations of the mean and maximum temperature of the heater. All these fluctuations are in phase. When the heat flux increases, at a constant value of mass flux, the oscillation amplitudes of the pressure drop, the fluid and the heater temperatures also increased.

The large heated wall temperature fluctuations are associated with the critical heat flux (CHF). The CHF phenomenon is different from that observed in a single channel of conventional size channels. A key difference between micro-channel heat sink and single conventional channel is the amplification of the parallel-channel instability prior to CHF. As the heat flux approached CHF, the parallel-channel instability, which was moderate over a wide range of heat fluxes, became quite intense and should be associated with maximum temperature fluctuation of the heated surface. The dimensionless experimental values of heat transfer coefficient may be correlated using the Eotvos number and boiling number.

Acknowledgements

This research was supported by the Fund for Promotion of Research at the Technion. A. Mosyak is supported by a joint grant from the Center for Absorbtion in Science of the Ministry of Immigrant Absorbtion and the Committee for Planning and Budgeting of the Council for Higher Education under the framework of the KAMEA PROGRAM.

References

Bergles, A.E., Kandlikar, S.G., 2005. On the nature of critical heat flux in micro-channels. ASME J. Heat Transfer 127, 101–107.

Bergles, A.E., Lienhard, J.H., Kendall, E., Griffith, P., 2003. Boiling and evaporation in small diameter channels. Heat Transfer Eng. 24 (1), 18–40.

Dupont, V., Thome, J.R., Jacobi, A.M., 2004. Heat transfer model for evaporation in micro-channels. Part II: Comparison with the database. Int. J. Heat Mass Transfer 47, 3387–3401.

Guide to the Expression of Uncertainty of Measurement, Geneva, International Organization for Standardization, 1995.

Hetsroni, G., Mosyak, A., Segal, Z., 2001. IEEE Trans. Components Packag. Technol. 24, 16–23.

Hetsroni, G., Mosyak, A., Segal, Z., Ziskind, G., 2002. A uniform temperature heat sink for cooling of electronic devices. Int. J. Heat Mass Transfer 45, 3275–3286.

Hetsroni, G., Mosyak, A., Segal, Z., Pogrebnyak, E., 2003. Two-phase flow patterns in parallel micro-channels. Int. J. Multiphase Flow 29, 341–360.

Hetsroni, G., Yarin, L.P., Pogrebnyak, E., 2004. Onset of flow instability in a heated capillary tube. Int. J. Multiphase flow 30, 1421–1449.

Hetsroni, G., Mosyak, A., Pogrebnyak, E., Segal, Z., 2005. Explosive boiling of water in parallel micro-channels. Int. J. Multiphase Flow 31, 371–392.

Kakac, S., Veziroglu, T.N., 1983. A Review of two-phase flow instabilities. Advances in Two-phase Flow and Heat Transfer, vol. 11. Martinus Nijihoff, Boston, pp. 577–668.

Kakac, S., Veziroglu, T.N., Padki, M.M., Fu, L.Q., Chen, X.J., 1990. Investigation of thermal instabilities in a forced convection upward boiling system. Int. J. Exp. Thermal Fluid Sci. 3, 191–201.

Kandlikar, S.G., 1990. A general correlations for two-phase flow boiling heat transfer coefficient inside horizontal and vertical tubes. ASME J. Heat Transfer 112, 219–228.

Kandlikar, S.G., 2002. Fundamental issues related to flow boiling in mini-channels and micro-channels. Exp. Thermal Fluid Sci. 26, 389–407.

Kandlikar, S.G., 2004. Heat transfer mechanisms during flow boiling in micro-channels. J. Heat Transfer, Trans. ASME 126, 8–16.

Kandlikar, S.G., Balasubramanian, P., 2004. An extension of the flow boiling correlation to transition, laminar, and deep laminar flows in mini-channels and micro-channels. Heat Transfer Eng. 25 (3), 86–93.

Kew, P.A., Cornwell, K., 1997. Correlations for the prediction of pool boiling heat transfer in small diameter channels. Appl. Thermal Eng. 17, 705–717.

Lee, P.C., Tseng, F.G., Pan, C., 2004a. Bubble dynamics in micro-channels. Part I: Single micro-channel. Int. J. Multiphase Flow 47, 5575–5589.

Lee, P.C., Tseng, F.G., Pan, C., 2004b. Bubble dynamics in micro-channels. Part II: Two parallel micro-channels. Int. J. Multiphase Flow 47, 5591–5601.

Moriyama, K., Inoue, A., 1996. Thickness of the liquid film formed by a growing bubble in a narrow gap between two horizontal plates. J. Heat Transfer Trans. ASME 118, 132–139.

Qu, W., Mudawar, I., 2003a. Flow boiling heat transfer in two-phase micro-channel heat sinks-1 experimental investigation and assessment of correlation methods. Int. J. Heat Mass Transfer 46, 2755–2771.

Qu, W., Mudawar, I., 2003b. Flow boiling heat transfer in two-phase micro-channel heat sinks-2. Annular two-phase flow model. Int. J. Heat Mass Transfer 46, 2773–2784.

Steinke, M.E., Kandlikar, S.G., 2003. Flow boiling and pressure drop in parallel micro-channels. First International Conference on Micro-channels and Mini-channels. ASME, NY, pp. 567–579.

Steinke, M.E., Kandlikar, S.G., 2004. An experimental investigation of flow boiling characteristics of water in parallel micro-channels. ASME J. Heat Transfer 126, 518–526.

Thome, J.R., Dupont, V., Jacobi, A.M., 2004. Heat transfer model for evaporation in micro-channels. Part I: Presentation of the model. Int. J. Heat Mass Transfer 47, 3375–3385.

Wang, Q., Chen, X.J., Kakac, S., Ding, Y., 1994. An experimental investigation of density wave-type oscillations in a convection boiling upflow system. Int. J. Heat Fluid Flow 15, 241–246.

Wu, H.Y., Cheng, P., 2004. Boiling instability in parallel silicon micro-channels at different heat flux. Int. J. Heat Mass Transfer 47, 3631–3641.

Yao, S.C., Chang, Y., 1983. Pool boiling heat transfer in a confined space. Int. J. Heat Mass Transfer 26, 841–848.

Yen, T.H., Kasagi, N., Suzuki, Y., 2003. Forced convective boiling heat transfer in micro-tubes at low mass and heat fluxes. Int. J. Multiphase Flow 29, 1771–1792.

Zhang, L., Koo, J., Jiang, L., Asheghi, M., Goodson, K.E., Santiago, J.K., 2002. Measurements and modeling of two-phase flow in micro-channels with nearly constant heat flux boundary conditions. J. Microelectomech. Syst. 11, 12–19.